Optimisation of cutting parameters for improving energy efficiency in machining process

Luoke Hu[a], Renzhong Tang[a,c], Wei Cai[b,*](corresponding author), Yixiong Feng[a], Xiang Ma[d]

[a]*State Key Laboratory of Fluid Power and Mechatronic Systems, School of Mechanical Engineering, Zhejiang University, Hangzhou, 310027, China*

[b]*College of Engineering and Technology, Southwest University, Chongqing, 400715, China*

[c]*Key Laboratory of Advanced Manufacturing Technology of Zhejiang Province, School of Mechanical Engineering, Zhejiang University, Hangzhou, 310027, China*

[d]*Department of Metal Production and Processing, SINTEF Industry, P.O. Box 124 Blindern, N-0314 Oslo, Norway*

***Corresponding author:** Wei Cai.
E-mail address: weicai@swu.edu.cn (W. Cai).

Optimisation of cutting parameters for improving energy efficiency in machining process

Abstract: Reducing the machining energy consumption (MEC) of machine tools for turning operations is significant to promote sustainable manufacturing. It has been approved that selection of optimal cutting (turning) parameters is an effective approach to reduce the cutting energy consumption (CEC) within the MEC. However, the potentiality for this approach to reduce the non-cutting energy consumption (NCEC) has not received sufficient attentions. Especially, the energy consumed for spindle rotation change (SRCE) was neglected. Thus, this article aims at developing an integrated MEC model with NCEC and SRCE considered. Then, Simulated Annealing (SA) is employed to find the optimal spindle rotation speed (SRS) and feed rate which result in the minimum MEC. A case study is conducted, where five parts with different cutting lengths are processed on a lathe. The experiment results show that SA can obtain the global optimum in a short computation time when the step sizes for SRS and feed rate are 0.1 and 0.001, respectively. The optimal solution achieves a 19.28% MEC reduction. Finally, the relation between the part length and the optimal SRS is analysed, and the consequence of MEC minimisation on machining time is discussed.

Keywords: Cutting parameters selection; Turning operations; Non-cutting energy consumpton; Spindle rotation change; Machining energy optimisation; Simulated annealing.

1. Introduction

With the production and productivity increasing in modern society, the manufacturing energy consumption is increased with intensifying the energy crisis and global warming [1]. According to International Energy Agency [2], manufacturing is responsible for nearly 1/3 of the global energy consumption and 36% of carbon dioxide emissions [3]. Increasing energy price and requirements to improve energy efficiency are the severe challenges faced by modern manufacturing enterprises [4]. The statistics from the U.S. energy information administration [5] showed that machining energy consumption (MEC) of machine tools occupied more than 20% of total manufacturing energy consumption [6]. Turning, which is a conventional machining method for material removal, is widely used in manufacturing industries to produce rotational parts [7], with consuming a considerable proportion of MEC [8]. Thus, reducing MEC for turning operations is significant to promote the machining energy efficiency and alleviate the associated environmental issues [9].

The MEC can be comprised of different energy consumption and divided to two types: the cutting and non-cutting energy consumption (CEC and NCEC) [10]. The NCEC is the energy consumed for the non-cutting operations including tool path, tool change, and change of spindle rotation speed [11]. For the single-pass turning, the tool change is not required. The energy consumed when a part is actually cut by a machine tool is defined as the CEC [12]. It has been proved that changing cutting (turning) parameters (cutting speed, feed rate, and cutting depth) can lead to a large difference in CEC [13]. The investigation suggested that 6%-40% of the energy consumption can be changed through adjusting the cutting parameters (CPs) [14]. Thus, selecting the optimal CPs which results in the minimum CEC is considered as an effective energy saving approaches. However, the potentiality for the CPs optimisation approach to reduce the NCEC has not received attentions. Generally, the NCEC accounts for more than 30% of the total MEC [15]. The CPs can also affect the value of the NCEC, because the non-cutting parameters that affect the energy consumed for tool path (TPE) and spindle rotation change (SRCE) vary with the CPs. The SRCE can be subdivided into energy consumed for the spindle acceleration (SAE) and deceleration (SDE).

The TPE is defined as the energy consumed by the machine tool for moving the cutter to the right position to begin the actual cutting [16]. The SRCE is defined as the energy consumed by the machine tool when the spindle rotates from a low (high) speed to a high (low) speed [11]. The SRCE accounts for nearly 14% of the total NCEC and has energy-saving potentials [15]. For the NCEC, models of TPE and SRCE have been developed by Hu et al. [11] for solving the energy-related operation sequencing (OSeq) problem. In CPs selection, the optimisation of NCEC can lead to the

increase of CEC [17], thereby weakening the reduction of MEC. Thus, it is required to achieve the optimal trade-off between NCEC and CEC to minimise the total MEC.

According to the above analysis, our study aims at analysing the conflict between the NCEC and the CEC in single-pass turning, and at developing the integrated MEC model for the CPs optimisation problem. In this model, the objective functions describe the mathematic relation between the turning parameters and the MEC value, and the constraint equations restrict the values of turning parameters to guarantee the machining quality and the machine tool capability. Especially, the design parameters such as the length and diameter of the part have been included in the model. For single-pass turning, the cutting depth is considered as a constant because the initial and finished diameters of the part have been determined at its design phase. In terms of single objective optimisation, the aim is to determine the optimal turning parameters including spindle rotation speed (SRS) and feed rate which result in the minimum MEC under the machining constraints. A meta-heuristic, Simulated Annealing (SA), is modified and used as the optimisation approach, and is compared with Enumeration Method (EM) to validate its performance in solution quality and computation speed. Based on case studies, the proposed approach is demonstrated, compared, and discussed.

In the remainder of this paper, the literature review is presented in the next section. The description of the research problem and the MEC model are given in Section 3. In Section 4, the working procedures of SA for solving the optimisation problem are described. A case study is conducted to demonstrate the model and optimisation approach in Section 5. In Section 6, the optimisation results are compared, analysed, and discussed, followed by a brief summary and future work in Section 7.

2. Literature review

In recent ten years, an increasing amount of research has been conducted to reduce the MEC of machine tools through process planning, including CPs optimisation and OSeq. In the field of energy-related OSeq, Hu et al. [16] sequenced the machining operations for a part to minimise the NCEC considering the TPE. For the part with features interacting, the CEC models for milling and drilling were developed and integrated with the NCEC model to optimise the total MEC [10]. To improve the modelling efficiency, the MEC for the machining activities which are not affected by the operation sequence was identified and excluded [18]. The aforementioned approach cannot be directly applied to our CPs optimisation problem, because the OSeq problem is discrete and the sequence is the decision variable. Our problem is continuous and a combination of CPs is the

decision variable. Besides, the CEC model for turning has not been developed in the existing OSeq research.

Based on the experiments, Newman et al. [13] analysed the energy-related CPs optimisation problem for the computer numerical control (CNC) machining, and tested the effect of feed rate and cutting depth on the MEC in the case of cutting aluminium. However, the mathematic relation between the MEC and the CPs has not been provided. Box et al. proposed the response surface methodology (RSM) for determining the relation between the various process parameters and the dependent variables [19]. The regression model was obtained to calculate the energy consumed for cutting the 7075 aluminium alloy by a specific CNC turning machine [20]. Furthermore, Lv et al. improved the accuracy of the MEC model for turning by considering the standby, coolant spray, spindle rotation and feeding operations of machine tools, and the accuracy achieved to above 93% [21]. Zhong et al. [22] compared the MEC model of Lv et al. [21] with other models and validated its superiority in applicability, accuracy, and data collection. Thus, the model in Ref. [21] will be employed and modified to be suitable for the CPs optimisation problem. Based on the MEC model, the Taguchi technique was introduced to identify that feed rate and cutting depth are the most significant factors for influencing the MEC [17]. For single-pass turning, the cutting depth was given [23], and only the cutting speed and feed rate can be changed to reduce the MEC.

In above MEC models, only the CEC has been modelled while the NCEC was ignored. Consequently, the follow-up optimisation of CEC can lead to the increase of NCEC, thereby weakening the reduction of MEC. For example, it has been approved that the CEC can be minimised by selecting the maximum CPs such as the SRS [17]. However, the maximum SRS can lead to very large SRCE in NCEC, which probably results in the increase of the total MEC [24]. To bridge this knowledge gap, Li et al. [25] supplemented the NCEC model and obtained an integrated MEC model for the CPs optimisation problem. In the research on the MEC with the NCEC included, there are three limitations. (i) The NCEC for the activities which are not affected by the CPs has not been identified and excluded. It harms the modelling efficiency. (ii) The SRCE, which accounts for 14% of the total NCEC, has been neglected. Consequently, the CPs resulting in the high SRCE tend to be selected as the optimum. (iii) The design parameters can affect the selection of CPs for minimising the MEC, but they have not been included in the MEC model [26].

After developing the model, the algorithms can be employed to search for the optimal CPs that result in the minimum MEC. Hu et al. [10] have proved the effectiveness of Genetic Algorithm (GA) to solve the discrete energy-related OSeq problem. For the continuous CPs optimisation problem, the

performance of GA was not guaranteed. The specific algorithms to minimise the MEC in turning have received little attention. For solving the time-related or quality-oriented CPs optimisation problems, many algorithms including deterministic algorithms and meta-heuristics have been successful employed. These works can be used as references to select and use the algorithms. Traditionally, the deterministic algorithms such as integer programming [27] were used to find the optimal CPs which result in the minimum machining time and surface roughness [28]. Normally, these algorithms are only suitable for solving the small-to-medium sized problems, because the computation time is intolerant when the number of CPs schemes is huge. Meta-heuristics have become popular because they consume a short computation time for large problems. Their probabilities for finding the global optima are different for different problems. Hence, it is required to select a suitable meta-heuristic for a given problem. Yusup et al. [29] reviewed several meta-heuristics for solving the time-related CPs optimisation problem from 2007 to 2011, and it verified that SA can effectively solve this continuous problem and perform better than GA in terms of the solution quality [30]. Therefore, SA is chosen as an optimisation approach for minimising the MEC and is compared with the EM to validate its performance.

According to the literatures reviewed, the following research gaps have motivated our research. (i) The TPE and SRCE models in Ref. [11] and Ref. [16] cannot be directly employed, because the OSeq problem is discrete whereas our CPs optimisation problem is continuous. (ii) The NCEC for the activities which are not affected by the CPs has not been identified and excluded [18]. (iii) In CPs selection, the optimisation of NCEC can lead to the increase of CEC [17], thereby weakening the reduction of total MEC. Thus, it is required to achieve the optimal trade-off between NCEC and CEC to minimise the total MEC [10]. (iv) The effects of design parameters such as the part length on the selection of CPs for minimising the MEC have not been considered. Our article aims to bridge these research gaps. It is novel to minimise the MEC with NCEC, SRCE, and design parameters considered through the CPs optimisation, and the proposed model and optimisation approach are the main contributions. The integrated MEC model including objective functions and constraints and the optimisation approach based on SA are presented in following sections.

3. Problem description and modelling

The effect of CPs in turning operations on the MEC is investigated. In **Fig. 1**, a rotational part A machined by a lathe is used as an example to explain the CEC, the NCEC, and the possible conflict between them when the CPs are changed.

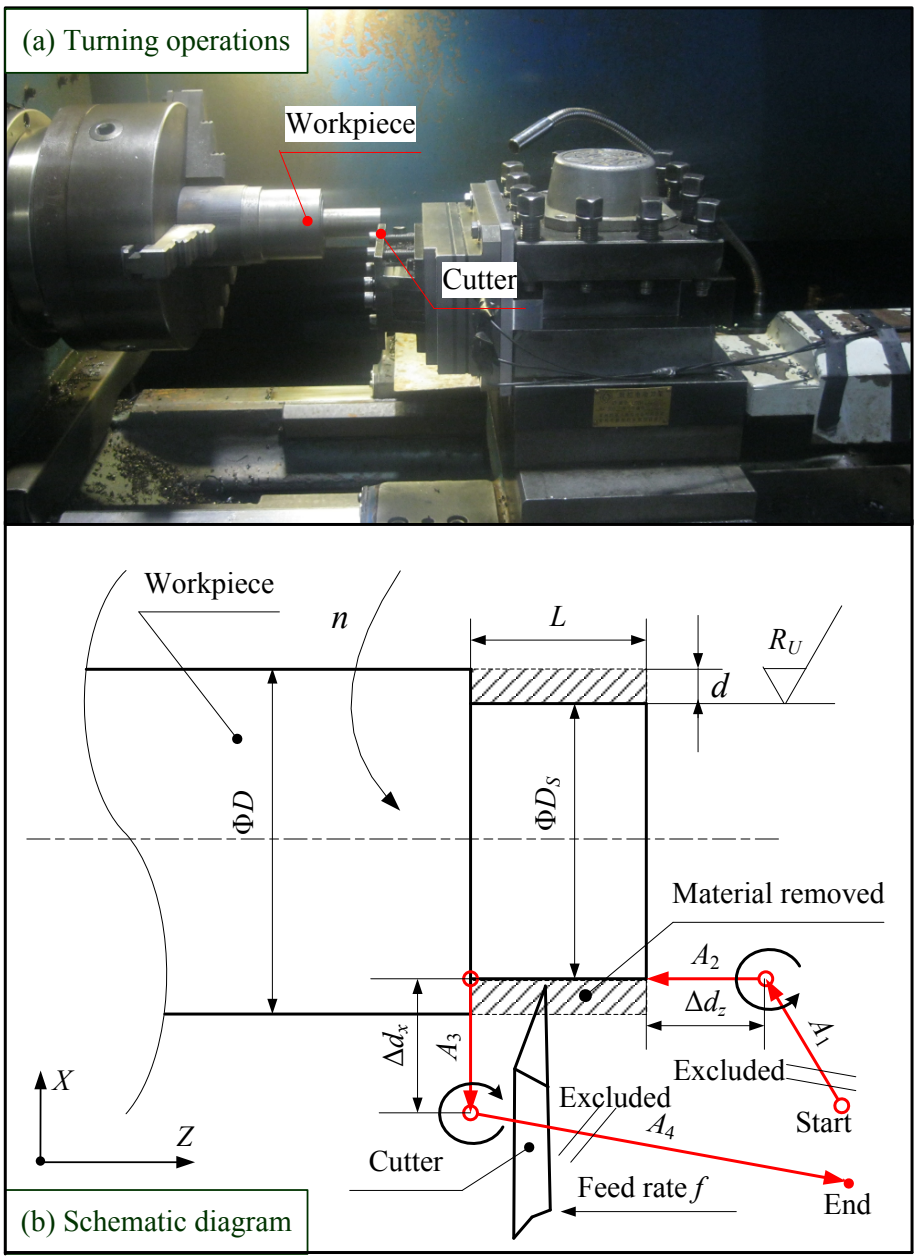

Fig. 1. Single-pass turning operations for a part.

Two schemes of CPs including SRS and feed rate for processing part A can be adopted: (a) 720rpm and 0.25mm/r; (b) 1080rpm and 0.25mm/r. In single-pass turning, the tool path is labelled by red arrowed lines, and the spindle acceleration and deceleration are marked as "↻" and "↺", as shown in **Fig. 1(b)**. The power profiles of the machine tool based on the aforementioned two schemes of CPs are shown in **Fig. 2**. The power profiles are developed based on the measured data and the prediction method by Jia [15] and Dahmus et al. [31].

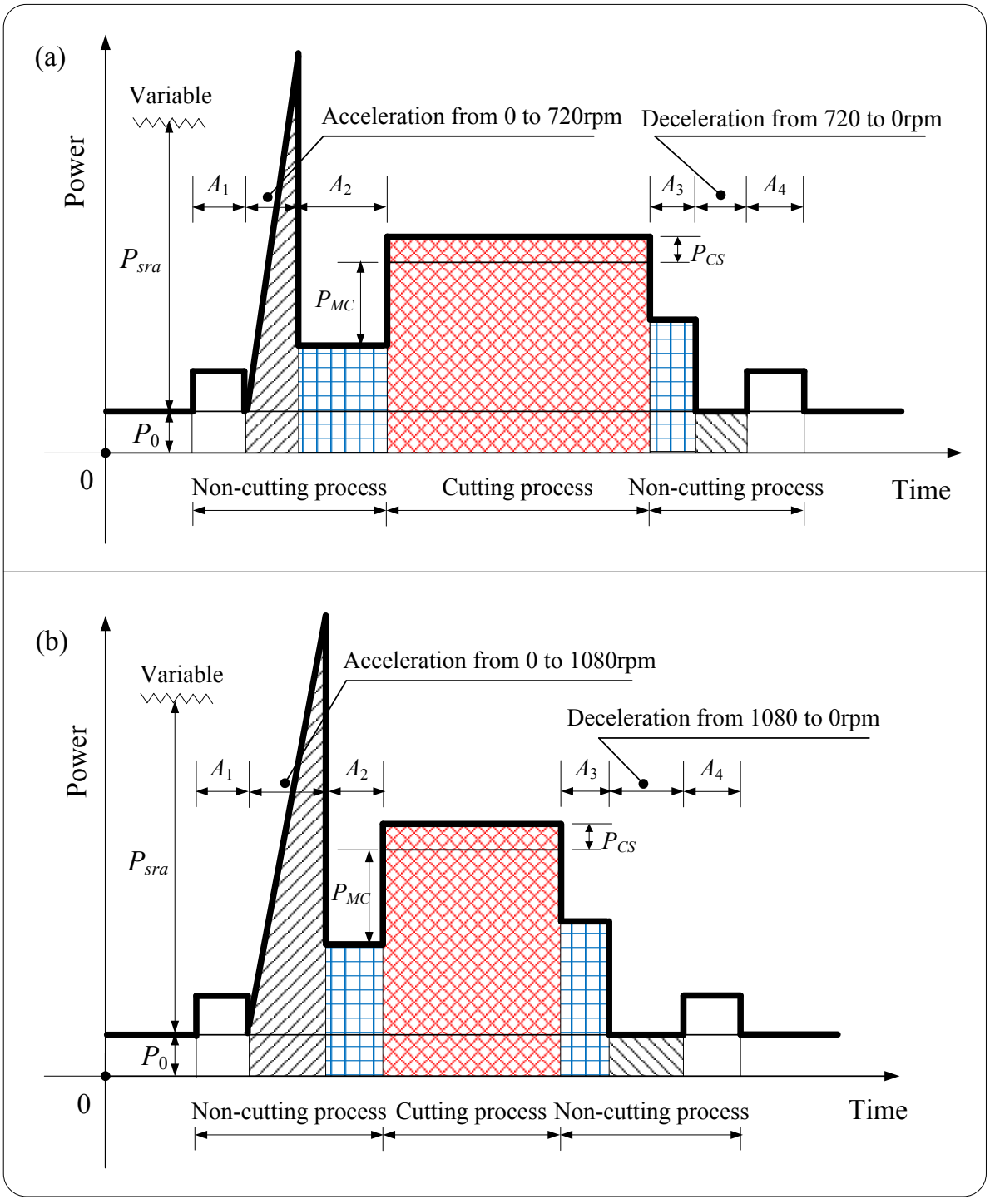

Fig. 2. Power profiles of two schemes of CPs: (a) 720rpm and 0.25mm/r; (b) 1080rpm and 0.25mm/r.

The first step is to identify and exclude the machining activities that are not affected by the CPs. In single-pass turning, there are four non-cutting feeding activities (A_1, A_2, A_3, and A_4), as shown in **Fig. 1(b)**. The feeding approaches for the 1-st and 4-th activities are rapid, and the spindle rotation speeds for them are set as 0 rpm to save MEC. Thus, the CPs cannot affect the energy consumed for these two activities [18]. In other words, their energy consumption cannot be reduced by changing the CPs.

The MEC for the 1-st and 4-th activities is excluded, and is filled with blank in **Fig. 2**. The areas filled with forward slashes and back slashes represent SAE and SDE, respectively, and the blue grids areas represent TPE, and the red nets areas represent CEC. By comparing the sizes of filled areas in **Fig. 2(a)** and **(b)**, it shows that different schemes of CPs can result in different values of CEC and NCEC.

The possible conflict between NCEC and CEC in single-pass turning is analysed. Because the SRS of the 1-st scheme (720rpm) is lower than that of the 2-nd one (1080rpm), the CEC for the 1-st scheme is larger than that for the 2-nd scheme due to its longer cutting time [17], as shown in **Fig. 2**. When only the CEC was considered in previous research, the 2-nd scheme whose SRS is higher was regarded as the more energy-efficient option. However, the NCEC for the 1-st scheme is smaller than that for the 2-nd scheme because low SRS consumes less SRCE, as shown in **Fig. 2**. If the increment of NCEC exceeds the decrement of CEC for the 2-nd scheme due to the high SRS, the 1-st scheme should be the better option. This example demonstrates the requirement to develop an integrated MEC model with NCEC and CEC included and select the suitable SRS to achieve the minimisation of total MEC. The 2-nd scheme can contribute to reducing more cutting time if the part length is increased. The cutting time is associated with the CEC. Thus, the design parameters such as the part length should be included in the MEC model.

3.1. Objective functions of the model

Following the example, the integrated MEC model for single-pass turning based on the CPs is developed. The objective function of the model can be expressed as:

$$minimise\ E_{total} = E_{cut} + E_{non} \tag{1}$$

where E_{total} is the total MEC of a machine tool for single-pass turning. E_{cut} and E_{non} are the CEC and the NCEC, respectively, which are modelled in Sections 3.1.1 and 3.1.2.

3.1.1. Cutting energy consumption (E_{cut})

For single-pass turning, the cutting power is a constant in the cutting process, as shown in **Fig. 2**. Thus, E_{cut} is modelled as:

$$E_{cut} = P_{cut} \times T_{cut} \tag{2}$$

where P_{cut} is the cutting power of the machine tool in turning [W], and T_{cut} is the cutting time [s]. P_{cut} can be divided to five portions: material removal power, *Z*-axial feeding power, spindle rotation power, coolant spray power, and standby power [22]. Standby power and coolant spray power are constant and remain the same while selecting different CPs. Material removal power, *Z*-axial feeding power, and spindle rotation power are variable. Thus, P_{cut} is expressed as:

$$P_{cut} = P_{MC} + P_{ZF} + P_{SR} + P_{CS} + P_0 \tag{3}$$

where P_{MC}, P_{ZF}, and P_{SR} are material removal power, *Z*-axial feeding power, and spindle rotation power, respectively. P_{CS} and P_0 are coolant spray power and standby power of the machine tool, as shown in **Fig. 2**, which are obtained by actual measurement.

In Expression (3), P_{MC} is developed according to a turning power model in Ref. [32], which considers the additional load losses and has high reliability, as below:

$$P_{MC} = C_M \cdot v^{w_M} \cdot f^{y_M} \cdot d^{x_M} \tag{4}$$

where C_M is the coefficient in the material removal power model; v, f, and d are cutting speed [m/min], feed rate [mm/r], and cutting depth [mm], respectively, in turning operations; w_M, y_M and x_M are the exponents of cutting speed, feed rate, and cutting depth, respectively. The coefficient and exponents are obtained by statistical analysis based on experiment data. In Equation (4), v is calculated by:

$$v = \frac{\pi \times (D - d) \times n}{1000} \tag{5}$$

where n is the SRS in the cutting process [rpm], and D is the initial diameter of the workpiece [mm].

By comparing several models for the *Z*-axial feeding power [22], a quadratic model in Ref. [15], which has the highest accuracy, is employed as:

$$P_{ZF} = A_{ZF} \times (v_F)^2 + B_{ZF} \times v_F + C_{ZF} \tag{6}$$

where A_{ZF}, B_{ZF}, and C_{ZF} are the quadratic coefficient, monomial coefficient, and constant in the model, which can be obtained by quadratic regression based on experiment data. v_F is the feeding speed [mm/min], which is calculated as:

$$v_F = n \times f \tag{7}$$

In Expression (3), an accurate linear equation in Ref. [33] is employed to model the P_{SR}, as follows:

$$P_{SR} = B_{SR} \times n + C_{SR} \tag{8}$$

where B_{SR} and C_{SR} are the monomial coefficient and constant in the spindle rotation power model, which are obtained by linear regression based on the experiment data.

In Expression (2), T_{cut} is calculated as:

$$T_{cut} = \frac{60 \times L}{v_F} \tag{9}$$

where L is the cutting length of the workpiece [mm].

3.1.2. Non-cutting energy consumption (E_{non})

For single-pass turning, the non-cutting process consists of tool path and change of SRS, as shown in **Fig. 1**. Thus, E_{non} is modelled as:

$$E_{non} = E_{TP} + E_{SRC} \tag{10}$$

where E_{TP} and E_{SRC} are TPE and SRCE, respectively, in single-pass turning. There are four feeding activities in a turning pass, as shown in **Fig. 1(b)**. The modelling for the 1-st and 4-th feeding activities are not required, thus E_{TP} can be expressed as:

$$E_{TP} = E_{TP}^2 + E_{TP}^3 \tag{11}$$

where E_{TP}^2 and E_{TP}^3 are TPE for the 2-nd and 3-rd feeding activities. The feeding approach for the 2-nd feeding activity is normal with the SRS of n rpm, and the feeding direction is Z-axial. According to the model in Ref. [16], E_{TP}^2 is expressed as:

$$E_{TP}^2 = P_{TP}^2 \times t_2 = (P_0 + P_{SR} + P_{ZF}) \times \frac{60 \times \Delta d_z}{v_F} \tag{12}$$

where P_{TP}^2 and t_2 are the power and time of the machine tool for the 2-nd feeding activity, respectively; Δd_z is the air-cutting distance before actually cutting the material [mm].

The feeding approach for the 3-rd feeding activity is rapid, and the feeding direction is *X*-axial. Thus, E_{TP}^{3} is expressed as:

$$E_{TP}^{3} = P_{TP}^{3} \times t_3 = (P_0 + P_{SR} + P_{XR}) \times \frac{60 \times \Delta d_x}{1000 \times v_{XR}} \tag{13}$$

where P_{TP}^{3} and t_3 are the power and time of the machine tool for the 3-rd feeding activity, respectively; P_{XR} represents the rapid feeding power of *X*-axis [W]; v_{XR} is the rapid feeding speed of *X*-axis [m/min]; Δd_x is the retracting distance of the tool in *X*-axis [mm].

In single-pass turning, the SRS accelerates from 0 rpm to n rpm and finally decelerates from n rpm to 0 rpm. Thus, E_{SRC} is expressed as:

$$E_{SRC} = E_{sra} + E_{srd} \tag{14}$$

where E_{sra} and E_{srd} represent the energy consumption of the machine tool for the spindle rotation acceleration from 0 rpm to n rpm and for the spindle rotation deceleration from n rpm to 0 rpm, respectively. According to the model in Ref. [11], E_{sra} is expressed as:

$$E_{sra} = \int_0^{t_{sra}} (P_0 + P_{sra}) dt \tag{15}$$

where P_{sra} is the power of the spindle system in the spindle acceleration from 0 rpm to n rpm [W]; t_{sra} is the time for the spindle acceleration [s]. The model in Ref. [24] is employed to model the P_{sra} as:

$$P_{sra} = B_{SR} \times \left(\frac{30\alpha_A t}{\pi}\right) + C_{SR} + T_s \times (\alpha_A t) \tag{16}$$

where α_A and T_s are the angular acceleration [rad/s^2] and acceleration torque [N·m] of a spindle, respectively, which are obtained by experiment measurements.

In Expression (15), t_{sra} is calculated by:

$$t_{sra} = \frac{2\pi n}{60\alpha_A}. \tag{17}$$

For a spindle deceleration, no power is consumed by the spindle system normally, and only standby power is consumed [11]. Thus, E_{srd} is expressed as:

$$E_{srd} = P_0 \times t_{srd} \tag{18}$$

where t_{srd} is the time for the spindle deceleration from n rpm to 0 rpm [s], which is calculated by:

$$t_{srd} = \frac{-2\pi n}{60\alpha_D} \tag{19}$$

where α_D is the angular deceleration [rad/s^2].

3.2. Constraint equations of the model

In actual CPs selection, the feed rate and SRS selected must satisfy all constraint equations of the model. According to Ref. [34], the constraint equations are developed considering (1) CPs limits as well as the maximum allowable (2) SRS, (3) cutting force, (4) cutting power, and (5) surface roughness. They are described as follows.

(1) CPs constraints

The CPs constraints are expressed in terms of lower and upper bounds. The feed rate constraint is expressed as:

$$f_L \le f \le f_U \tag{20}$$

where f_L and f_U are lower and upper bounds of feed rates, respectively, in turning [mm/r].

The SRS constraint converts from the cutting speed constraint, as below:

$$\begin{cases} v_L \le v \le v_U \\ v = \dfrac{\pi \times (D-d) \times n}{1000} \end{cases} \overset{\text{Conversion}}{\Rightarrow} \frac{1000 v_L}{\pi \times (D-d)} \le n \le \frac{1000 v_U}{\pi \times (D-d)} \tag{21}$$

where v_L and v_U are lower and upper bounds of cutting speeds, respectively, in turning [m/min]. The bounds on feed rate and cutting speed are related to the material of workpiece and the type of cutting tool [35].

(2) Maximum allowable SRS constraint

The SRS selected should not exceed the maximum SRS value allowed by the machine tool. This constraint is expressed as:

$$n \le n_{max} \tag{22}$$

where n_{max} is the maximum allowable SRS of a machine tool [rpm], which is obtained from the machine specification.

(3) Cutting force constraint

When selecting large CPs, the cutting force can increase [36]. To limit the machining deflection of the workpiece and cutting tool [36], the cutting force F_{cut} should be restricted to a certain maximum value F_U. Based on the cutting force model in Ref. [37], the cutting force constraint is:

$$F_{cut} = C_Q \cdot v^{w_Q} \cdot f^{y_Q} \cdot d^{x_Q} \leq F_U \tag{23}$$

where F_U is the maximum allowable cutting force [N], which is determined by the stability and strength of the machine and the cutting tool [37]; C_Q is the coefficient in the cutting force model; w_Q, y_Q and x_Q are exponents of cutting speed, feed rate, and cutting depth, respectively, in the cutting force model [14]. The coefficient and exponents are obtained by statistical analysis based on experiment data [37].

(4) Cutting power constraint

During the cutting process, the cutting power P_{cut} should not exceed the maximum available power of the machine [38]. Based on the cutting power model in Expression (3), the cutting power constraint is:

$$P_{cut} \leq P_U \tag{24}$$

where P_U is the maximum available power of the machine [W], which is obtained from the machine specification [28].

(5) Surface roughness constraint

The surface roughness is an important index to reflect the surface quality of the machined part [39], and should not exceed the maximum allowable value [35]. The surface roughness is generally influenced by various parameters such as CPs, tool geometry, tool material, and tool wear [35]. Narang et al. proved that feed rate and nose radius have the most dominant effects on surface roughness [40]. Following Lin et al. [41], the surface roughness constraint is expressed as:

$$\frac{f^2}{8R_N} \leq R_U \tag{25}$$

where R_U is the maximum allowable surface roughness [μm], which is given by the technical criteria [37], and R_N is the nose radius of the cutting tool [mm].

4. Single objective optimisation

After developing the integrated model, SA is selected as the optimisation approach to search for the optimal SRS and feed rate, by using the minimisation of MEC as the objective. SA can avoid being trapped in local optima and is able to explore globally for more possible solutions. Thus, the global optimum is more likely to be obtained by SA. However, as a probabilistic optimisation technique, it is not guaranteed that SA always gets the global optimum due to the nature of meta-heuristics [42]. Hence, the EM, which is a deterministic approach for the MEC minimisation, is used as the benchmark for the verification of the performance of SA in Section 5. EM is a procedure to list all feasible combinations of the variables of SRS and feed rate under the Constraints (20)-(25), and then to calculate the corresponding objective values of MEC according to Expressions (1)-(19) one by one [43]. By comparison, the combination of the two variables that results in the minimum MEC is selected as the optimum.

SA is a meta-heuristic that simulates the process of annealing in metallurgy to bring the system, from an arbitrary initial state, to a ground state with the minimum internal energy [42]. It was invented by Kirkpatrick et al. [44] in 1983. The simulation of annealing can be used to find an approximation of a global minimum for a function with a number of variables [44]. The candidate solution is generated by performing the random perturbations on the old solution and is checked to be accepted or not according to the energy (objective value) difference in each iteration at each temperature. A stochastic criterion regarding the acceptance of worse solutions is incorporated to prevent the algorithm from being prematurely trapped in local optima [45]. After cooling to the end temperature, the global optimal or near-optimal solutions to the optimisation problem are generated.

According to Expressions (1)-(19), the objective function merely varies with SRS and feed rate, as below:

$$E_{total} = g(n, f) \tag{26}$$

Based on the flowchart of SA in **Fig. 3**, the working procedures for minimising the E_{total} through selecting the values of n and f are described as follows. The performance of SA in solution quality is improved by developing the memory function that avoids losing the excellent solution.

Step 1: The cooling schedule is specified, including the initial temperature T_0, the temperature decrease function $T_k = h(k)$, the end temperature T_e, and the length of Markov chain L_c. An initial solution $\begin{cases} n = n_0 \\ f = f_0 \end{cases}$ is random generated from the feasible solution space, and the iteration number is $k = 0$.

Step 2: A memory matrix M and a memory function G are developed and added to the standard SA. At the beginning, the solution $\begin{cases} n = n_0 \\ f = f_0 \end{cases}$ is recorded in the matrix M, and the memory function is $G = g(n_0, f_0)$.

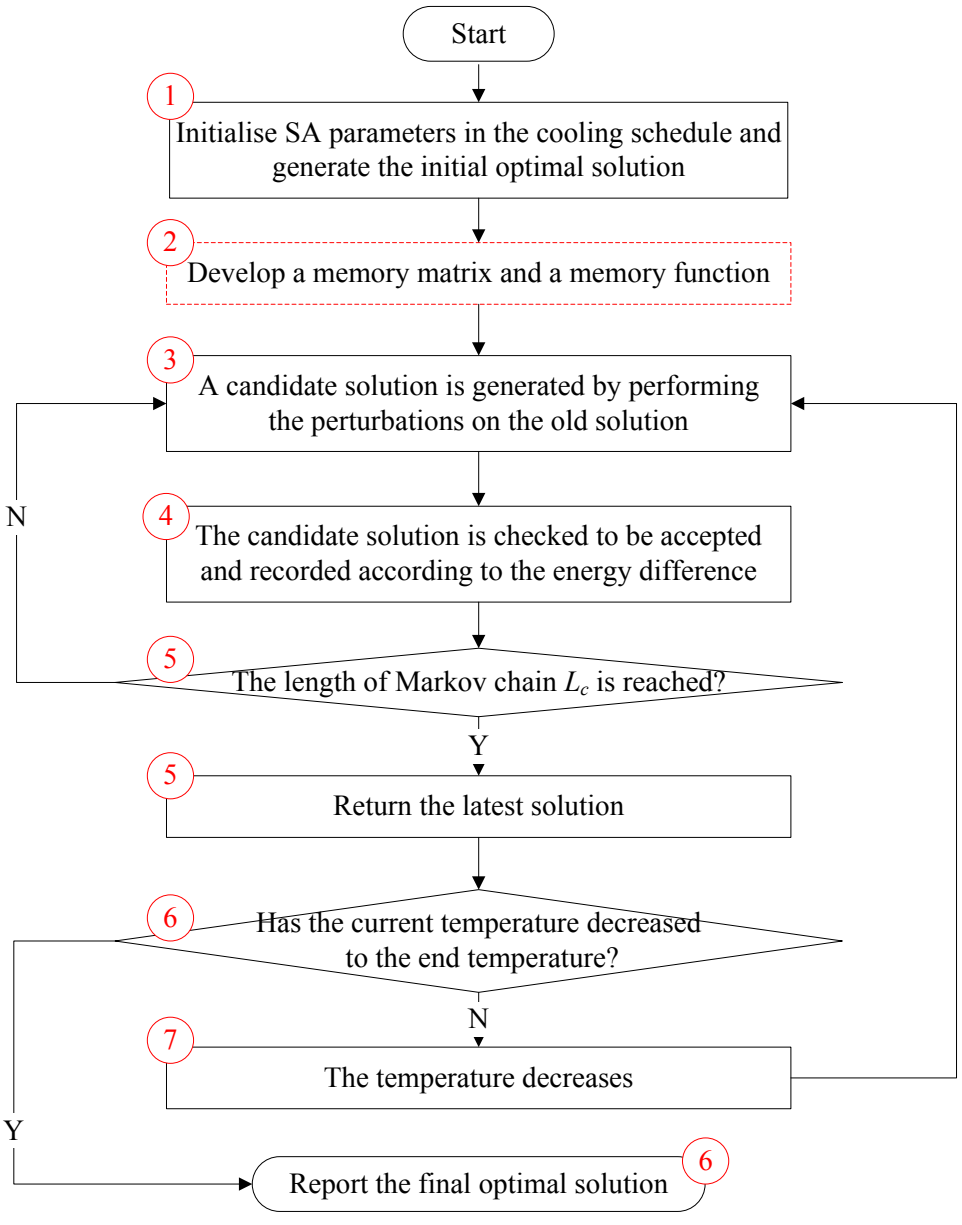

Fig. 3. A flowchart of Simulated Annealing (SA).

Step 3: The random perturbations Δn and Δf about SRS and feed rate are performed on the last solution n and f. A candidate solution is generated by operating $n = n + \Delta n$ and $f = f + \Delta f$. If the candidate solution violates the Constraints (20)-(25), Δf is changed to $\Delta f = -\Delta f$. If still violating the constraints, Δn is further changed to $\Delta n = -\Delta n$.

Step 4: If the candidate solution is better than the existing solution $g(n, f) \geq g(n + \Delta n, f + \Delta f)$, it is directly accepted as the new optimal solution. Moreover, $g(n + \Delta n, f + \Delta f)$ is compared with the memory function G. If $g(n + \Delta n, f + \Delta f) < G$, the function is changed to $G = g(n + \Delta n, f + \Delta f)$, and the solution $\begin{cases} n = n + \Delta n \\ f = f + \Delta f \end{cases}$ is recorded in the matrix M.

If $g(n, f) < g(n + \Delta n, f + \Delta f)$, the acceptance of the worse solution depends on the Metropolis criterion [46]. For instance, if $exp\left(\frac{g(n,f) - g(n + \Delta n, f + \Delta f)}{T_k}\right) > \text{random}[0,1)$, then $\begin{cases} n = n + \Delta n \\ f = f + \Delta f \end{cases}$ is accepted as the new optimal solution. Otherwise, it is rejected.

Step 5: If Steps 3 and 4 have been performed L_c times at the temperature T_k, SA returns the latest solution and goes to Step 6. Otherwise, SA returns to Step 3.

Step 6: If the current temperature T_k has decreased to the end temperature T_e ($T_k \leq T_e$), SA stops. Otherwise, Step 7 is performed. After SA stops, the optimal solution is compared with the solutions in the matrix M, and the solution with the minimum MEC is selected as the final solution.

Step 7: The number of iterations is operated by $k = k + 1$, and the returned solution in Step 5 is regarded as the last solution. The temperature decreases to T_{k+1}, and SA returns to Step 3.

The performance of SA for optimising the MEC for the parts with different design parameters is tested in Section 5.

5. Case study

A part A, as shown in **Fig. 1**, is used in this case study. The part is made of 45#Steel. Its length L and diameter D_S are 20.5mm and 38.6mm, respectively, and the diameter D is 42.4mm. The maximum allowable surface roughness is R_U=2.7μm. A CNC lathe (CK6153i) manufactured by Jinan First Machine Tool Co., Ltd. of China is employed to process this part. The cutting tool for turning is VNMG160408, and its nose radius is R_N=0.8mm. The experiment setup for the power data collection

on the CK6153i is shown in **Fig. 4**, and the experiment method is described in Ref. [21]. The key parameters of the CK6153i required for the MEC model are listed in **Table 1**. Dry cutting is adopted and the coolant spray switch is OFF, thus the corresponding power is P_{CS}=0W. **Table 2** lists the coefficients and exponents in the material removal power model and cutting force model under specific cutting conditions. They have been obtained by experiment measurements and regression analyses based on the experiment data [32]. The process parameters for part A are listed in **Tables 3**, which are obtained from the process files.

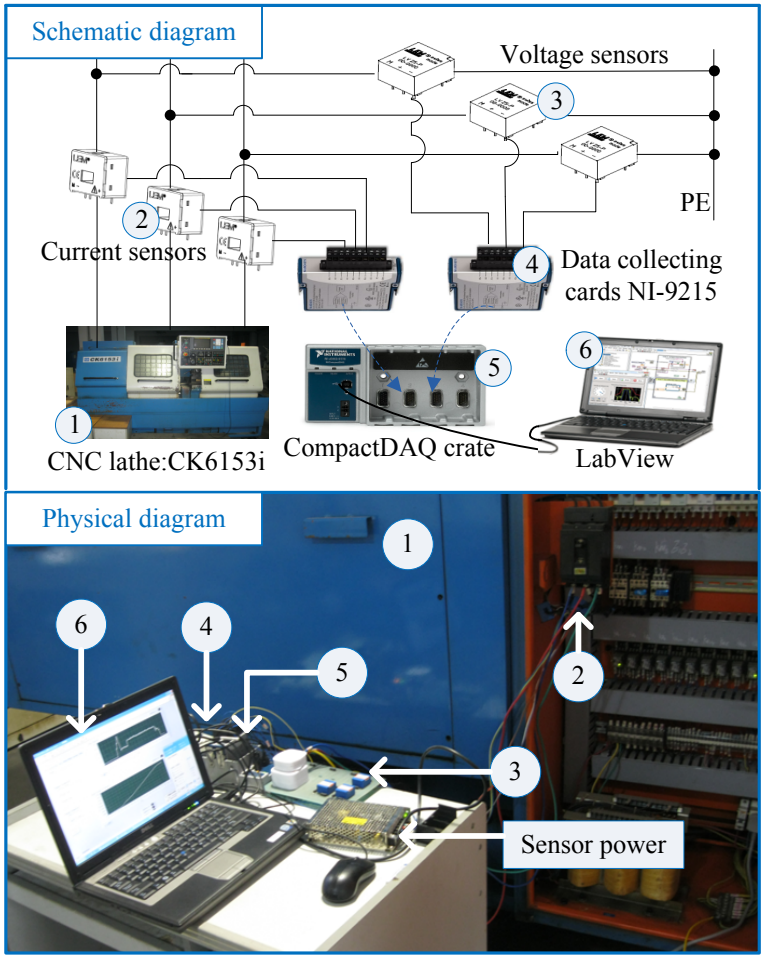

Fig. 4. A diagram of experiment setup for the power data acquisition.

Table 1 Parameters of the CNC lathe (CK6153i) in the MEC model.

Parameter	Notation [Unites]	Value
Standby power	P_0 [W]	332.1
Coolant spray power (ON, OFF)	P_{CS} [W]	(369.5, 0)
Monomial coefficient and constant in the spindle rotation power model	(B_{SR}, C_{SR})	(1.09, 41.12)

Quadratic coefficient, monomial coefficient, and constant in the feeding power model of *Z*-axis	(A_{ZF}, B_{ZF}, C_{ZF})	$(2.32\times10^{-6}, 0.030, 0.49)$
Angular acceleration and deceleration of the spindle	(α_A, α_D) [rad/s^2]	(39.78, -38.79)
Acceleration torque of the spindle	T_s [N·m]	28.42
Rapid feeding speed of *X*-axis	v_{XR} [m/min]	4
Rapid feeding power of *X*-axis	P_{XR} [W]	135.0
Maximum allowable SRS	n_{max} [rpm]	2000
Maximum available power of the machine tool	P_U [W]	7500

Table 2 Coefficients and exponents in the cutting models for part A.

Coefficient/exponent	Value
Coefficient in the material removal power model C_M	44.57
Exponent of cutting speed, feed rate, and cutting depth in the material removal power model (w_M, y_M, x_M)	(0.909, 0.657, 0.917)
Coefficient in the cutting force model C_Q	2355
Exponent of cutting speed, feed rate, and cutting depth in the cutting force model (w_Q, y_Q, x_Q)	(-0.0724, 0.655, 0.902)

Table 3 Process parameters for part A.

Parameter	Notation [Unites]	Value
Cutting length and depth in turning	(L, d) [mm]	(10.5, 1.9)
Retracting distance of the tool in *X*-axis	Δd_x [mm]	4.0
Air-cutting distance before actually cutting	Δd_z [mm]	5.0
Maximum allowable surface roughness	R_U [μm]	2.7
Lower and upper bounds of cutting speed	(v_L, v_U) [m/min]	(85, 170)
Lower and upper bounds of feed rate	(f_L, f_U) [mm/r]	(0.100, 0.350)

Maximum allowable cutting force	F_U [N]	1280

Based on above data and the Expressions (1)-(25), the energy consumed by the CK6153i for processing part A with arbitrary values of SRS and feed rate is modelled. The objective function is:

$$minimise\ E_{total} = E_{cut} + E_{non} = \left[\left(P_{MC} + P_{ZF} + P_{SR} + 0 + 332.1\right) \times \frac{60 \times 20.5}{n \times f}\right] + \left(E_{TP} + E_{SRC}\right)$$

where:

$$P_{MC} = 44.57 \cdot \left(\frac{\pi \times 40.5 \times n}{1000}\right)^{0.909} \cdot f^{0.657} \cdot 1.9^{0.917},$$

$$P_{ZF} = 2.32 \times 10^{-6} \times (n \times f)^2 + 0.030 \times n \times f + 0.49,$$

$$P_{SR} = 1.09 \times n + 41.12,$$

$$E_{TP} = \left(332.1 + P_{SR} + P_{ZF}\right) \times \frac{60 \times 5.0}{n \times f} + \left(332.1 + P_{SR} + 135.0\right) \times \frac{60 \times 4.0}{1000 \times 4},$$

$$E_{SRC} = \int_0^{\frac{2\pi n}{60 \times 39.78}} \left[332.1 + 1.09 \times \left(\frac{30 \times 39.78 \times t}{\pi}\right) + 41.12 + 28.42 \times 39.78 \times t\right] dt + 332.1 \times \frac{-2\pi n}{60 \times (-38.79)}.$$

The constraint equations are:

$$0.100 \le f \le 0.350,$$

$$\frac{1000 \times 85}{\pi \times 40.5} \le n \le \frac{1000 \times 170}{\pi \times 40.5},$$

$$n \le 2000,$$

$$2355 \cdot \left(\frac{\pi \times 40.5 \times n}{1000}\right)^{-0.0724} \cdot f^{0.655} \cdot 1.9^{0.902} \le 1280,$$

$$P_{MC} + P_{ZF} + P_{SR} + 0 + 332.1 \le 7500,$$

$$\frac{f^2}{8 \times 0.8} \le 2.7.$$

Two algorithms, including EM and SA, are employed as optimisation approaches. They are developed on Dev C++ 5.11.0 software with the programming language C++. The computing platform is: Intel (R) Core (TM) i7-2630 QM CPU with 2.00 GHz frequency, 4.00 GB RAM, and Windows 7 (64bit) operating system. According to the machining accuracy of CK6153i, the step sizes for n and f in the algorithms are set to 0.1 and 0.001, respectively. The EM returns the global minimum MEC for part A, which is 26460.6J. A computation time of EM is 0.751 seconds, and the optimal values of SRS and feed rate are: $n = 668.1\text{rpm}$ and $f = 0.266\text{mm/r}$.

The parameter values used for SA are obtained by tuning, and their values are as follows: the initial temperature $T_0 = 200$, the temperature decrease function $T_k = T_0 \times 0.98^k$, the end temperature $T_e = 0.001$, and the length of Markov chain $L_c = 100$. By running SA for 50 times, it achieves the global minimum MEC of 26460.6J in all trials for part A, which is excellent. An average computation time of SA is 0.130 seconds, and the corresponding CPs are the same as that produced by EM. A searching process of SA for the global optimum is shown in **Fig. 5**. For this specific problem, SA usually converges within 300 iterations, and there is no premature convergence happening. The comparisons of EM and SA for part A in the 50 trials are summarised in **Table 4**.

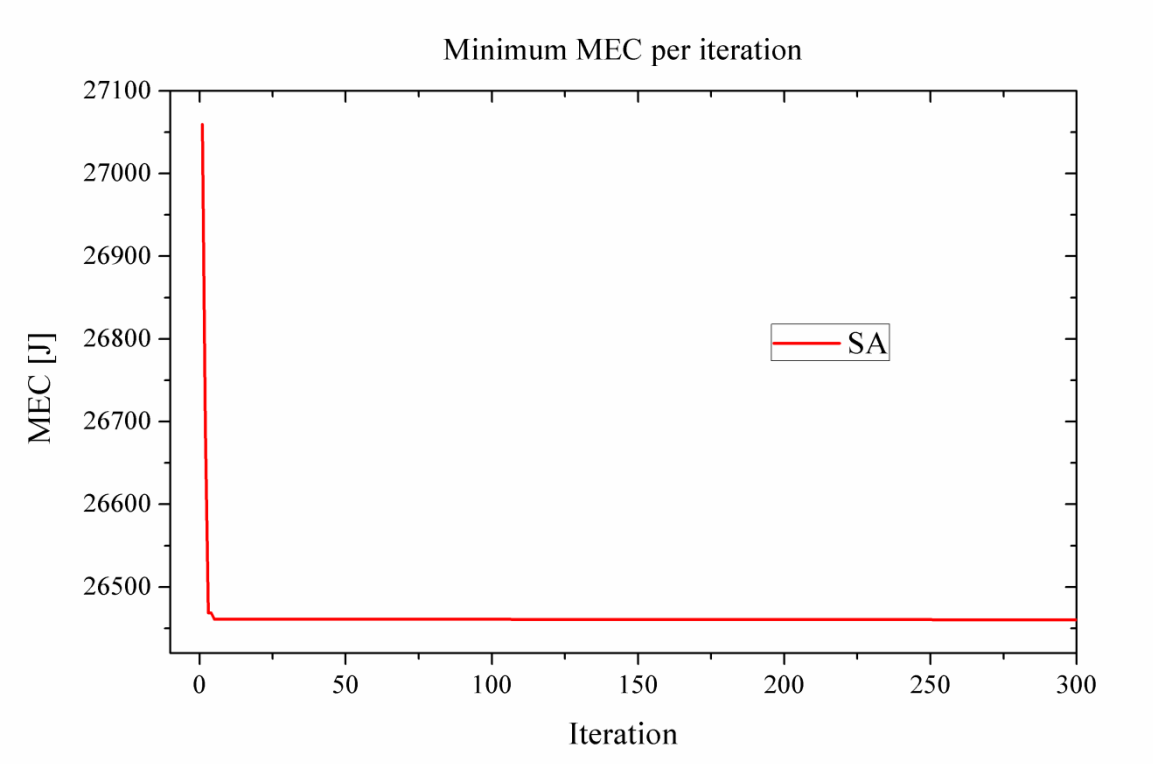

Fig. 5. A searching process of SA for the optimal solution of part A.

The developed approaches are further tested and validated on four parts B, C, D, and E with the length L of 20.6mm, 105.8mm, 191.0mm, and 191.1mm, respectively. Their diameters D_S and D are 38.6mm and 42.4mm. The results from using EM and SA for optimising the CPs of these parts are compared and summarised in **Table 4**. According to **Table 4**, the minimum MEC, the optimal SRS, and the optimal feed rate are changed with the part length. The optimisation results obtained by SA and EM are exactly same for every part, and it suggests that SA still has a 100% probability of finding the global optima. Hence, SA performs as well as EM in solution quality for all cases. In terms of computation time, SA outperforms EM. Specifically, the computation time of SA is approximately 82.69% [(0.751-0.130)/0.751] shorter than that of EM for part A. In sum, SA is recommended for our problem because it can effectively return the global optima in a short computation time.

Table 4 The comparisons of EM and SA for five parts.

Part names			Part A	Part B	Part C	Part D	Part E
Length of the part			20.5	20.6	105.8	191.0	191.1
Algorithms	EM	Minimum MEC achieved [J]	26460.6	26562.2	106264.2	181241.1	181328.8
		Optimal SRS [rpm]	668.1	687.3	1240.2	1335.8	1336.1
		Optimal feed rate [mm/r]	0.266	0.267	0.285	0.287	0.287
		Computation time [s]	0.751	0.750	0.751	0.750	0.749
	SA	Minimum MEC achieved [J]	26460.6	26562.2	106264.2	181241.1	181328.8
		Optimal SRS [rpm]	668.1	687.3	1240.2	1335.8	1336.1
		Optimal feed rate [mm/r]	0.266	0.267	0.285	0.287	0.287
		Percent of getting minimum	100%	100%	100%	100%	100%
		Median MEC of 50 trials [J]	26460.6	26562.2	106264.2	181241.1	181328.8
		Computation time [s]	0.130	0.129	0.133	0.138	0.140

6. Discussion

In the case study, the proposed CPs optimisation approach for minimising MEC has been demonstrated, and the optima have been efficiently obtained by SA. In this section, the optimisation results are compared, analysed, and discussed.

6.1. Energy savings benefit from the proposed approach

To demonstrate the effectiveness of the proposed approach in reducing the MEC, the following comparison is conducted. High SRS with medium feed rate (or HSMF for short) technique serves as the benchmark to represent the traditional approach to arranging the CPs [47]. In HSMF, the high

SRS can reduce the cutting time while the medium feed rate can guarantee the surface quality. For example, the values of SRS and feed rate for parts A and C, generated by the HSMF, are $n = 1300$ rpm and $f = 0.25\text{mm/r}$. The corresponding MEC is 32779.9J and 113979.4J, respectively. Although the HSMF can improve the material removal rate and surface quality, our approach can reduce 19.28% [(32779.9-26460.6)/32779.9] and 6.77% [(113979.4-106264.2)/113979.4] of MEC for parts A and C, respectively. A higher percent of MEC for part A is saved than that of part C, because the optimal SRS of part C (1240.2rpm) is much closer to the benchmark (1300rpm) than that of part A (668.1rpm) and the energy-saving potential of part C is restricted.

6.2. Relation between the part length and the optimal SRS

In traditional CPs optimisation for minimising the MEC, only the cutting process is concerned while the spindle rotation change is neglected. In actual machining, the spindle rotation change is inevitable with consuming considerable energy. After considering it, the optimisation results indicate a positive correlation between the part length and the optimal SRS, as shown in **Fig. 6**. According to **Fig. 6**, the optimal SRS increases from the lower bound 668.1rpm to the upper bound 1336.1rpm, with the part length increased from 20.5mm to 191.1mm. From 105.8mm to 191.1mm, the optimal SRS slowly increases. Specifically, the increase rate of the optimal SRS from 191.0mm to 191.1mm [(1336.1-1335.8)/(191.1-191.0)=3] is much smaller than that from 20.5mm to 20.6mm [(687.3-668.1)/(20.6-20.5)=192]. This suggests that the relation is not linear. Based on more experiments and tests, as shown in **Fig. 6**, the optimal SRS for any part shorter than 20.5mm is 668.1rpm, and the optimal SRS for any part longer than 191.1mm is 1336.1rpm. For the short part, although the high SRS can help reduce the CEC, more NCEC will be sacrificed for the spindle rotation acceleration and deceleration. In sum, the shorter the part is, the lower the SRS should be selected for balancing NCEC and CEC to realise the minimisation of total MEC.

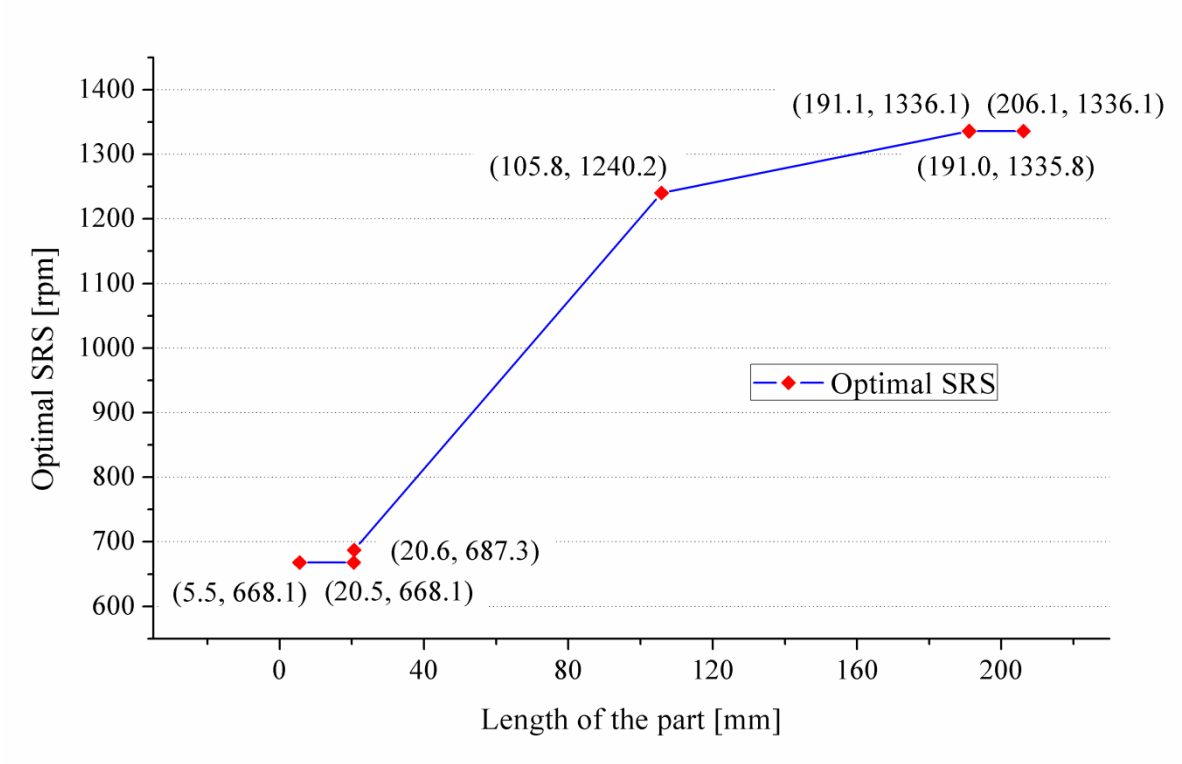

Fig. 6. The relation between the part length and the optimal SRS.

6.3. Consequence of MEC minimisation on machining time

In a real manufacturing scenario, it is not reasonable to optimise the MEC with largely sacrificing the machining time, thereby causing a machine tardiness problem. The consequence of MEC minimisation on machining time is analysed and discussed. According to Expressions (9), (12), (13), (17), and (19), the machining time for single-pass turning (T_{total}) is calculated as:

$$T_{total} = \frac{60 \times L}{n \times f} + \frac{60 \times \Delta d_z}{n \times f} + \frac{60 \times \Delta d_x}{1000 \times v_{XR}} + \frac{2\pi n}{60\alpha_A} + \frac{-2\pi n}{60\alpha_D}.$$

For example, the machining time based on the optima of parts A ($n = 668.1\text{rpm}$ and $f = 0.266$ mm/r) and C ($n = 1240.2\text{rpm}$ and $f = 0.285\text{mm/r}$) is 12.23 seconds and 25.48 seconds, respectively. By comparison, the CPs of parts A and C without the MEC consideration are generated by the aforementioned HSMF technique, and the machining time based on these CPs ($n = 1300\text{rpm}$ and $f = 0.25\text{mm/r}$) is 11.70 seconds and 27.45 seconds for parts A and C, respectively. For part C, 7.18% [(27.45-25.48)/27.45] of the machining time reductions benefit from the MEC minimisation. However, 4.53% [(12.23-11.70)/11.70] of the machining time increases suffer from the MEC minimisation for part A, and this verifies the conflict between the machining time and energy consumption. Thus, when optimising the CPs for a specific part, it is required to make a trade-off

between the reductions of machining time and energy consumption. For part A, the optimal parameters ($n = 668.1\text{rpm}$ and $f = 0.266\text{mm/r}$) can be adopted if 4.53% of the machining time increases are acceptable.

6.4. Effect of step sizes of CPs on the MEC optimisation

If step sizes for n and f are allowed to be set to the smaller values than 0.1 and 0.001, more MEC can be reduced. For example, when step sizes for n and f are decreased to 0.01 and 0.0001, the minimum MEC from using EM for part B is decreased from 26562.2J to 26553.7J. The optimal SRS considerably decreases from 687.3rpm to 668.87rpm, and the optimal feed rate slightly decreases from 0.267mm/r to 0.2662mm/r. The computation time of EM sharply increases from 0.750 seconds to 74.282 seconds. By comparison, the computation time of SA is only 0.132 seconds. With the step sizes decreased, the probability of SA to find the global optimum (26553.7J) decreases to 12%, and SA frequently returns a near-optimum due to the nature of meta-heuristics. The median MEC that was obtained by SA for part B is 26553.9J, and the solution quality of SA is only 0.000753% [(26553.9-26553.7)/26553.7] inferior to that of EM. However, the computation time of SA is 99.82% [(74.282-0.132)/74.282] less than that of EM. When the step sizes are further decreased, the superiority of SA in terms of the computation time will become more prominent. In sum, SA is still recommended when the step sizes are small, because it requires much less computation time with little sacrifice in solution quality.

7. Conclusions and future work

Reducing the MEC for turning operations can play a significant role in promoting manufacturing energy efficiency and alleviating the associated environmental issues. It has been confirmed that the CEC within the MEC can be effectively reduce by selecting the optimal turning parameters at the process planning stage. However, the NCEC portion has not been well explored in previous research. Especially, the effect of CPs on the SRCE was neglected, and the SRCE normally accounts for 14% of the total NCEC. In this article, the conflict between NCEC and CEC in single-pass turning has been verified, and the integrated MEC model with NCEC and SRCE included has been developed. In this model, the unrelated machining activities have been excluded to improve the modelling efficiency, and the design parameters of the part have been considered. The single objective optimisation problem that minimises the total MEC is introduced, and SA is modified as the optimisation approach to search for the optimal SRS and feed rate. SA is compared with EM to validate its solution quality and computation time. In summary, it is novel to minimise the MEC with

the NCEC, the SRCE, and the design parameters considered through CPs optimisation, and the proposed model and optimisation approach are the main contributions.

In the case study, five rotational parts with different cutting lengths are processed by a CNC lathe (CK6153i). According to the optimisation results, SA has 100% probability of finding the global optima when the step sizes for SRS and feed rate are 0.1 and 0.001. The computation time of SA is 82.69% shorter than that of EM for a case. Thus, SA is effective for solving our specific problem. By using the approach, 19.28% and 6.77% MEC can be reduced for parts A and C, respectively. The relation between the part length and the optimal SRS is analysed, and it suggests that the lower SRS should be selected for the shorter part to save more MEC. Moreover, the consequence of MEC minimisation on machining time is discussed, and it shows that the MEC minimisation may lead to the machining time increase. Thus, a trade-off between the reductions of machining time and energy consumption should be made. Finally, it verifies that more MEC can be saved when the step sizes for SRS and feed rate are set to the smaller values than 0.1 and 0.001.

In this presented article, the model is merely suitable for single-pass turning. When the cutting depth is large, multi-pass turning is required. The model should be improved for the multi-pass turning, through developing the sub-model for the subdivision of cutting depth. Furthermore, the model can be improved by considering more constraints, including tool-life, spindle torque, stable cutting region, and chip-tool interface temperature. One limitation of the research is that other machining operations, such as milling and drilling, have not been considered. These operations are widely used in manufacturing and have energy-saving potential. For the next step, the energy consumed for these operations will be modelled and optimised. More cases with different combinations of machining conditions, such as machine tools and materials, will be studied to prove the generality of our research work. The single objective is another limitation. In actual manufacturing, it is unreasonable to only reduce the MEC without controlling the machining time, quality, and cost. For the next step, multi-objective optimisation approach will be employed to obtain the optimal CPs that result in the optimal trade-off among the aforementioned objectives. In the future, the proposed CPs optimisation approach will be combined with the existing OSeq optimisation to promote the energy-efficient integrated process planning. Finally, the approach will be developed on product design software such as SolidWorks, Pro/E, UG, and CATIA to assist in industrial applications.

Acknowledgments

The authors would like to thank the support from the National Natural Science Foundation of China (Grant No. 51805479) and the Research Committee of UM (Grant No. MYRG2018-00087-FBA).

Appendix A. Abbreviations and notations

The abbreviations and notations used in the problem statement, the algorithm description and throughout the paper are as follows:

	Abbreviations
CEC	cutting energy consumption [J]
CNC	computer numerical control
CPs	cutting parameters
EM	enumeration method
GA	genetic algorithm
HSMF	high SRS with medium feed rate
MEC	machining energy consumption [J]
NCEC	non-cutting energy consumption [J]
OSeq	operation sequencing
rpm	revolutions per minute
SA	simulated annealing
SAE	energy consumed for spindle acceleration [J]
SDE	energy consumed for spindle deceleration [J]
SRCE	energy consumed for spindle rotation change [J]
SRS	spindle rotation speed [rpm]
TPE	energy consumed for tool path [J]

	Nomenclature
α_A	angular acceleration of a spindle [rad/s^2]
α_D	angular deceleration of a spindle [rad/s^2]
A_{ZF}, B_{ZF}, C_{ZF}	quadratic coefficient, monomial coefficient, and constant in the Z-axial feeding power model
B_{SR}, C_{SR}	monomial coefficient and constant in the spindle rotation power model
C_M	coefficient in the material removal power model
C_Q	coefficient in the cutting force model
d	cutting depth in turning operations [mm]
D	initial diameter of the workpiece [mm]
D_S	finished diameter of the workpiece [mm]
E_{cut}	CEC for single-pass turning operations [J]
E_{non}	NCEC for single-pass turning operations [J]
E_{sra}	energy consumption of the machine tool for the spindle rotation acceleration from 0 rpm to n rpm [J]
E_{srd}	energy consumption of the machine tool for the spindle rotation deceleration from n rpm to 0 rpm [J]
E_{SRC}	SRCE in single-pass turning operations [J]
E_{total}	total MEC of a machine tool for single-pass turning operations [J]
E_{TP}	TPE in single-pass turning operations [J]

E_{TP}^2, E_{TP}^3	TPE for the 2-nd and 3-rd feeding activities in single-pass turning operations [J]
f	feed rate in turning operations [mm/r]
f_0	feed rate when the iteration number is 0 [mm/r]
f_L	lower bound of feed rate in turning [mm/r]
f_U	upper bound of feed rate in turning [mm/r]
F_{cut}	cutting force [N]
F_U	maximum allowable cutting force [N]
g	MEC function
G	memory function
h	temperature decrease function
k	index for the iteration
L	cutting length of the workpiece [mm]
L_c	length of Markov chain
M	memory matrix
n	SRS in the cutting process [rpm]
n_0	SRS when the iteration number is 0 [rpm]
n_{max}	maximum allowable SRS of the machine tool [rpm]
P_0	standby power of the machine tool [W]
P_{cut}	cutting power in turning operations [W]
P_{CS}	coolant spray power of the machine tool [W]
P_{MC}	material removal power [W]
P_{sra}	power of the spindle system in the spindle acceleration from 0 rpm to n rpm [W]
P_{SR}	spindle rotation power [W]
P_{TP}^2, P_{TP}^3	power of the machine tool for the 2-nd and 3-rd feeding activities [W]
P_U	maximum available power of the machine tool [W]
P_{XR}	rapid feeding power of *X*-axis [W]
P_{ZF}	*Z*-axial feeding power [W]
R_N	nose radius of the cutting tool [mm]
R_U	maximum allowable surface roughness [μm]
t_2, t_3	time of the machine tool for the 2-nd and 3-rd feeding activities [s]
t_{sra}	time for the spindle acceleration from 0 rpm to n rpm [s]
t_{srd}	time for the spindle deceleration from n rpm to 0 rpm [s]
T_0	initial temperature
T_{cut}	cutting time in turning operations [s]
T_e	end temperature
T_k	temperature in k-th iteration
T_s	acceleration torque of a spindle [N·m]
T_{total}	total machining time of a machine tool for single-pass turning operations [s]
v	cutting speed in turning [m/min]
v_F	feeding speed in turning [mm/min]
v_L	lower bound of cutting speed in turning [m/min]
v_U	upper bound of cutting speed in turning [m/min]
v_{XR}	rapid feeding speed of *X*-axis [m/min]
w_M, y_M, x_M	exponents of cutting speed, feed rate, and cutting depth, respectively, in the material removal power model
w_Q, y_Q, x_Q	exponents of cutting speed, feed rate, and cutting depth, respectively, in the cutting force model
Δd_x	retracting distance of the tool in *X*-axis [mm]
Δd_z	air-cutting distance before actually cutting the material [mm]
Δn	random perturbation about SRS on the last solution n [rpm]
Δf	random perturbation about feed rate on the last solution f [mm/r]

References

[1] T. Spiering, S. Kohlitz, H. Sundmaeker, C. Herrmann, Energy efficiency benchmarking for injection moulding processes, Robot. and Comput.-Integr. Manuf. 36 (2015) 45-59.

[2] IEA, Tracking industrial energy efficiency and CO_2 emissions, 2007; Available at: https://www.iea.org/publications/freepublications/publication/tracking_emissions.pdf [accessed June 2, 2018].

[3] W. Cai, K. Lai, C. Liu, F. Wei, M. Ma, S. Jia, Z. Jiang, L. Lv, Promoting sustainability of manufacturing industry through the lean energy-saving and emission-reduction strategy, Sci. Total Environ. 665 (2019) 23-32.

[4] O.V. Arriaza, D. Kim, D.Y. Lee, M.A. Suhaimi, Trade-off analysis between machining time and energy consumption in impeller NC machining, Robot. and Comput.-Integr. Manuf. 43 (2017) 164-170.

[5] EIA, Annual energy review 2011, 2012; Available at: http://www.eia.gov/totalenergy/data/annual/index.cfm [accessed July 3, 2018].

[6] L. Zhou, J. Li, F. Li, Q. Meng, J. Li, X. Xu, Energy consumption model and energy efficiency of machine tools: a comprehensive literature review, J. Clean. Prod. 112 (2016) 3721-3734.

[7] M. Givehchi, A. Haghighi, L. Wang, Cloud-DPP for distributed process planning of mill-turn machining operations, Robot. and Comput.-Integr. Manuf. 47 (2017) 76-84.

[8] L. Hu, R. Tang, K. He, S. Jia, Estimating machining-related energy consumption of parts at the design phase based on feature technology, Int. J. Prod. Res. 53 (2015) 7016-7033.

[9] W. Cai, C. Liu, C. Zhang, M. Ma, W. Rao, W. Li, K. He, M. Gao, Developing the ecological compensation criterion of industrial solid waste based on emergy for sustainable development, Energy 157 (2018) 940-948.

[10] L. Hu, C. Peng, S. Evans, T. Peng, Y. Liu, R. Tang, A. Tiwari, Minimising the machining energy consumption of a machine tool by sequencing the features of a part, Energy 121 (2017) 292-305.

[11] L. Hu, Y. Liu, N. Lohse, R. Tang, J. Lv, C. Peng, S. Evans, Sequencing the features to minimise the non-cutting energy consumption in machining considering the change of spindle rotation speed, Energy 139 (2017) 935-946.

[12] W. Cai, F. Liu, H. Zhang, P. Liu, J. Tuo, Development of dynamic energy benchmark for mass production in machining systems for energy management and energy-efficiency improvement, Appl. Energ. 202 (2017) 715-725.

[13] S.T. Newman, A. Nassehi, R. Imani-Asrai, V. Dhokia, Energy efficient process planning for CNC machining, CIRP J. Manuf. Sci. Tech. 5 (2012) 127-136.

[14] C. Li, Q. Xiao, Y. Tang, L. Li, A method integrating Taguchi, RSM and MOPSO to CNC machining parameters optimization for energy saving, J. Clean. Prod. 135 (2016) 263-275.

[15] S. Jia, Research on energy demand modeling and intelligent computing of machining process for low carbon manufacturing [dissertation], Zhejiang University, Hangzhou, (2014).

[16] L. Hu, Y. Liu, C. Peng, W. Tang, R. Tang, A. Tiwari, Minimising the energy consumption of tool change and tool path of machining by sequencing the features, Energy 147 (2018) 390-402.

[17] C. Camposeco-Negrete, Optimization of cutting parameters using Response Surface Method for minimizing energy consumption and maximizing cutting quality in turning of AISI 6061 T6 aluminum, J. Clean. Prod. 91 (2015) 109-117.

[18] L. Hu, R. Tang, Y. Liu, Y. Cao, A. Tiwari, Optimising the machining time, deviation and energy consumption through a multi-objective feature sequencing approach, Energ. Convers. Manage. 160 (2018) 126-140.

[19] G.E. Box, K.B. Wilson, On the experimental attainment of optimum conditions, in: Breakthroughs in statistics, Springer, 1992, pp. 270-310.
[20] R.K. Bhushan, Optimization of cutting parameters for minimizing power consumption and maximizing tool life during machining of Al alloy SiC particle composites, J. Clean. Prod. 39 (2013) 242-254.
[21] J. Lv, R. Tang, S. Jia, Y. Liu, Experimental study on energy consumption of computer numerical control machine tools, J. Clean. Prod. 112 (2016) 3864-3874.
[22] Q. Zhong, R. Tang, J. Lv, S. Jia, M. Jin, Evaluation on models of calculating energy consumption in metal cutting processes: a case of external turning process, Int. J. Adv. Manuf. Tech. 82 (2016) 2087-2099.
[23] B. Gopalakrishnan, F. Al-Khayyal, Machine parameter selection for turning with constraints: an analytical approach based on geometric programming, Int. J. Prod. Res. 29 (1991) 1897-1908.
[24] J. Lv, R. Tang, W. Tang, Y. Liu, Y. Zhang, S. Jia, An investigation into reducing the spindle acceleration energy consumption of machine tools, J. Clean. Prod. 143 (2017) 794-803.
[25] L. Li, C. Li, Y. Tang, L. Li, An integrated approach of process planning and cutting parameter optimization for energy-aware CNC machining, J. Clean. Prod. 162 (2017) 458-473.
[26] W. Cai, C. Liu, K. Lai, L. Li, J. Cunha, L. Hu, Energy performance certification in mechanical manufacturing industry: A review and analysis, Energ. Convers. Manage. 186 (2019) 415-432.
[27] R. Gupta, J. Batra, G. Lal, Determination of optimal subdivision of depth of cut in multipass turning with constraints, Int. J. Prod. Res. 33 (1995) 2555-2565.
[28] J. Wang, T. Kuriyagawa, X. Wei, D. Guo, Optimization of cutting conditions for single pass turning operations using a deterministic approach, Int. J. Mach. Tool. Manu. 42 (2002) 1023-1033.
[29] N. Yusup, A.M. Zain, S.Z.M. Hashim, Evolutionary techniques in optimizing machining parameters: Review and recent applications (2007–2011), Expert Syst. Appl. 39 (2012) 9909-9927.
[30] P. Asokan, R. Saravanan, K. Vijayakumar, Machining parameters optimisation for turning cylindrical stock into a continuous finished profile using genetic algorithm (GA) and simulated annealing (SA), Int. J. Adv. Manuf. Tech. 21 (2003) 1-9.
[31] J.B. Dahmus, T.G. Gutowski, An environmental analysis of machining, in: ASME 2004 international mechanical engineering congress and exposition, American Society of Mechanical Engineers, 2004, pp. 643-652.
[32] J. Lv, Research on energy supply modeling of computer numerical control machine tools for low carbon manufacturing [dissertation], Zhejiang University, Hangzhou, (2014).
[33] J. Lv, R. Tang, S. Jia, Therblig-based energy supply modeling of computer numerical control machine tools, J. Clean. Prod. 65 (2014) 168-177.
[34] C. Lu, L. Gao, X. Li, P. Chen, Energy-efficient multi-pass turning operation using multi-objective backtracking search algorithm, J. Clean. Prod. 137 (2016) 1516-1531.
[35] M. Chen, D. Tsai, A simulated annealing approach for optimization of multi-pass turning operations, Int. J. Prod. Res. 34 (1996) 2803-2825.
[36] S.B. Reddy, M. Shunmugam, T. Narendran, Optimal sub-division of the depth of cut to achieve minimum production cost in multi-pass turning using a genetic algorithm, J. Mater. Process. Tech. 79 (1998) 101-108.
[37] R.Q. Sardinas, M.R. Santana, E.A. Brindis, Genetic algorithm-based multi-objective optimization of cutting parameters in turning processes, Eng. Appl. Artif. Intel. 19 (2006) 127-133.
[38] Z. Deng, H. Zhang, Y. Fu, L. Wan, W. Liu, Optimization of process parameters for minimum energy consumption based on cutting specific energy consumption, J. Clean. Prod. 166 (2017) 1407-1414.

[39] J.W. Ahn, W.S. Woo, C.M. Lee, A study on the energy efficiency of specific cutting energy in laser-assisted machining, Appl. Therm. Eng. 94 (2016) 748-753.
[40] R. Narang, G. Fischer, Development of a framework to automate process planning functions and to determine machining parameters, Int. J. Prod. Res. 31 (1993) 1921-1942.
[41] W. Lin, D. Yu, C. Zhang, S. Zhang, Y. Tian, S. Liu, M. Luo, Multi-objective optimization of machining parameters in multi-pass turning operations for low-carbon manufacturing, P. I. Mech. Eng. Part B J. Eng. Manu. 231 (2017) 2372-2383.
[42] F. Musharavati, A.M.S. Hamouda, Simulated annealing with auxiliary knowledge for process planning optimization in reconfigurable manufacturing, Robot. and Comput.-Integr. Manuf. 28 (2012) 113-131.
[43] R. Gupta, K.S. Shishodia, G.S. Sekhon, Optimization of grinding process parameters using enumeration method, J. Mater. Process. Tech. 112 (2001) 63-67.
[44] S. Kirkpatrick, C.D. Gelatt, M.P. Vecchi, Optimization by simulated annealing, Science 220 (1983) 671-680.
[45] J.F.D. Martín, J.M.R. Sierra, A Comparison of Cooling Schedules for Simulated Annealing, in: Encyclopedia of Artificial Intelligence, IGI Global, 2009, pp. 344-352.
[46] P. Tian, J. Ma, D.M. Zhang, Application of the simulated annealing algorithm to the combinatorial optimisation problem with permutation property: An investigation of generation mechanism, Eur. J. Oper. Res. 118 (1999) 81-94.
[47] N.S. Kumar, A. Shetty, A. Shetty, K. Ananth, H. Shetty, Effect of spindle speed and feed rate on surface roughness of Carbon Steels in CNC turning, Procedia Eng. 38 (2012) 691-697.